Flow analysis for the Falkner–Skan wedge flow

H. Bararnia[1], N. Haghparast[1], Mo. Miansari[1,2,*] and A. Barari[3]

[1]Department of Mechanical Engineering, Babol University of Technology, P. O. Box 484, Babol, Iran
[2]Department of Mechanical and Aerospace Engineering, Monash University, Clayton, VIC 3800, Australia
[3]Department of Civil Engineering, Aalborg University, Sohngårdsholmsvej 57, 9000 Aalborg, Aalborg, Denmark

In this article an analytical technique, namely the homotopy analysis method (HAM), is applied to solve the momentum and energy equations in the case of a two-dimensional incompressible flow passing over a wedge. The trail and error method and Padé approximation strategies have been used to obtain the constant coefficients in the approximated solution. The effects of the polynomial terms of HAM are considered and the accuracy of the results is shown, which increases with the increasing polynomial terms of HAM. Analytical results for the dimensionless velocity and temperature profiles of the wedge flow are presented graphically for different values of the wedge angle and Prandtl number. Results show good accuracy when compared with the numerical solution.

Keywords: Homotopy analysis method, polynomial terms, thermal boundary-layer problem, wedge flow.

THE homotopy analysis method (HAM) is used to solve a wide range of physical problems, especially thermal boundary-layer problems, i.e. for two-dimensional incompressible and steady laminar flow passing over a wedge. These types of boundary-layer problems are expressed in the form of nonlinear third-order partial differential equations, which cannot be solved directly in a closed form. These equations were first mentioned by Falkner and Skan[1] in 1931 and hence are also called the Falkner–Skan equations. The solutions and their dependence on β were also later examined by Hartree[2]. Falkner and Skan[1] developed a similarity transformation method in which the partial differential boundary-layer equation. It also was reduced to a nonlinear third-order ordinary differential equation, which could then be solved numerically. Na[3] employed a group of transformations to reduce the third-order boundary value problem to a pair of initial value problems, and then solved these problems by means of a forward integration scheme.

Rajagopal *et al.*[4] studied the Falkner–Skan boundary-layer flow of a homogeneous incompressible second-grade fluid past a wedge placed symmetrically with respect to the flow direction. Lin and Lin[5] introduced a similarity solution method for the forced convection heat transfer from isothermal or uniform-flux surfaces to fluids of any Prandtl number. The solutions of the resulting similarity equations are given by the Runge–Kutta scheme. Hsu *et al.*[6] studied the temperature and flow fields of the flow past a wedge by the series expansion method, similarity transformation, Runge–Kutta integration and the shooting method. Asaithambi[7] presented a finite-difference method for solving the Falkner–Skan equation. Later, Hsu and Hsiao[8] presented a combination of a series expansion, similarity transformation and finite difference method for the heat transfer problem of a second-grade viscoelastic fluid past a plate fin. Bor-Lih Kuo[9] studied the heat transfer analysis for the Falkner–Skan wedge flow by the differential transformation method; the results were in a good agreement with those provided by other numerical methods.

The present study employs the HAM, which is one of the most powerful and useful methods for analytical solution with infinite boundary conditions (body flow). This method has an auxiliary coefficient ($\hbar$) for controlling the convergence of solution. As proposed by several authors[10–22], we have to solve these equations to higher orders, which can converge the solution to an appropriate range of $\hbar$. There have been several studies on this topic. In the present study, we have combined each method (trial and error or Padé approximation) with HAM. First, we show the efficiency of combination of HAM with the trial and error method for solving the momentum equation. We can also solve the momentum equation by combining the Padé approximation with HAM. For illustrating the efficiency of the Padé approximation, we also solve the momentum equation for the flat plate; the results are shown in Table 1. Then the energy equation is

Table 1. Padé approximation and $f''(0)$ for the case of $\beta = 0$ (flat plate)

Padé approximation	$f''(0)$	Error (%)
[2/2]	0.2	57.41
[4/4]	0.5188	10.47
[7/7]	0.4460	5.02
[9/9]	0.4798	2.17
[10/10]	0.4700	8.51E-2
[12/12]	0.4680	3.40E-1
[14/14]	0.4693	6.38E-2
[15/15]	0.4696	0.0
[16/16]	0.4696	0.0
[17/17]	0.4696	0.0

*For correspondence. (e-mail: morteza.miansarigavzan@monash.edu)

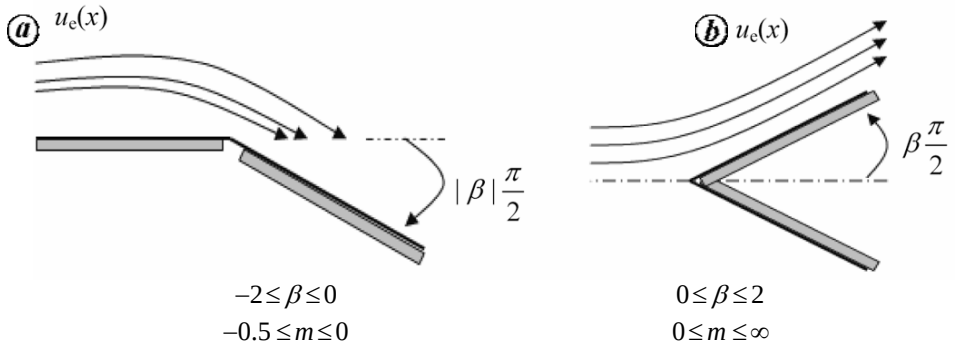

Figure 1. Different potential flows over a wedge. ***a***, Flow around a corner (diffusion). ***b***, Wedge flow.

solved with a combination of HAM and Padé approximation. In addition, the accuracy of results is strongly related to the number of HAM terms.

Physical analysis

The preceding analytical results are all based on the assumption that the pressure gradient term is negligible relative to inertia and friction in the boundary-layer momentum equation. This assumption applies to the case of a flat wall parallel to a uniform stream. If, as is shown in Figure 1 *b*, the wall makes a positive angle $\beta\frac{\pi}{2}$ with the free stream, then the free stream is accelerated in the *x*-direction along the wall (*x* is measured away from the tip of the wedge). Graphically, the acceleration of the flow is indicated by the gradual increase in the density of the streamline. Neglecting the laminar boundary layer in which viscosity balances inertia, the flow engulfing the wedge of angle $\beta\pi$ may be treated as inviscid and may be determined analytically based on potential flow theory. Note that the inviscid flow residing outside the laminar boundary layer is governed by the balance between inertia and pressure gradients.

Falkner–Skan flows

For the family of flows, we assume that the edge velocity $u_e(x)$, is of the following form

$$u_e(x) = Kx^m, \tag{1}$$

where *K* is an arbitrary constant. The pressure can be calculated from the Bernoulli in the outer inviscid flow

$$p_e + \frac{1}{2}\rho u_e^2 = \text{const}$$

$$\Rightarrow \frac{dp_e}{dx} = -\rho u_e \frac{du_e}{dx}$$

$$\Rightarrow \frac{dp_e}{dx} = -\rho K_m^2 x^{2m-1}$$

$$\text{If } m > 0, \text{ then } \frac{dp_e}{dx} < 0 \Rightarrow \text{ favourable pressure gradient.}$$

$$\text{If } m < 0, \text{ then } \frac{dp_e}{dx} > 0 \Rightarrow \text{ adverse pressure gradient.} \tag{2}$$

These edge velocities result from the following inviscid flows (Figure 1)

$$\beta \equiv \frac{2m}{m+1}.$$

Mathematical analysis

Considering the flow of an incompressible viscous fluid over a wedge (Figure 1 *b*), we find that the temperature of the wall, T_w, is uniform and constant, and is greater than the free stream temperature, T_∞. It is assumed that the free stream velocity, U_∞, is also uniform and constant. Further, assuming that the flow in the laminar boundary layer is two-dimensional and the temperature changes resulting from viscous dissipation are small, the continuity equation and the boundary-layer equations with $dp/dx = 0$, $f_x = 0$ and $u^m = 0$ may be expressed as

$$\frac{\partial u}{\partial x} + \frac{\partial v}{\partial y} = 0, \tag{3}$$

$$u\frac{\partial u}{\partial x} + v\frac{\partial u}{\partial y} = U\frac{\partial U}{\partial x} + \upsilon\frac{\partial^2 u}{\partial^2 y}, \tag{4}$$

$$u\frac{\partial T}{\partial x} + v\frac{\partial T}{\partial y} = \alpha\frac{\partial^2 T}{\partial^2 y}, \tag{5}$$

where u and v are the respective velocity components in the *x*- and *y*-directions of the fluid flow, υ the viscosity of

the fluid and U the reference velocity at the edge of boundary layer and is a function of x. α is the thermal diffusivity of the fluid, T the temperature in the vicinity of the wedge and boundary conditions are

$$\text{At} \quad y = 0: \quad u = v = 0 \text{ and } T = T_w,$$

$$\text{At} \quad y \to \infty: \quad u \to U(x) = U_\infty (x/L)^m \text{ and } T = T_\infty,$$

$$\text{At} \quad x = 0: \quad u = U_\infty \text{ and } T = T_\infty, \tag{6}$$

where U_∞ is the mainstream velocity, L the length of the wedge, m the Falkner–Skan power-law parameter and x measured from the tip of the wedge. A stream function, $\psi(x, y)$, is introduced such that

$$u = \frac{\partial \psi}{\partial y} \quad \text{and} \quad v = -\frac{\partial \psi}{\partial x}. \tag{7}$$

In addition to the physical considerations which require the introduction of this function, the mathematical significance of its use is that the equation of continuity, i.e. eq. (3) is satisfied identically. The momentum equation becomes

$$\frac{\partial \psi}{\partial y} + \frac{\partial^2 \psi}{\partial x\, \partial y} - \frac{\partial \psi}{\partial x}\frac{\partial^2 \psi}{\partial^2 y} = U\frac{\partial U}{\partial x} + \upsilon \frac{\partial^3 \psi}{\partial y^3}. \tag{8}$$

Integrating eq. (7) and introducing a similarity variable yields

$$f(\eta) = \sqrt{\frac{1+m}{2}\frac{L^m}{\upsilon U_\infty}} \cdot (\psi/(1+m)/2), \tag{9}$$

$$\eta = \sqrt{\frac{1+m}{2}\frac{U_\infty}{\upsilon L^m}} \cdot (y / x^{(1-m)/2}). \tag{10}$$

Substituting eqs (9) and (10) into eq. (8) gives

$$\frac{\mathrm{d}^3 f(\eta)}{\mathrm{d}\eta^3} + f(\eta)\frac{\mathrm{d}^2 f(\eta)}{\mathrm{d}\eta^2} + \beta\left[1 - \left(\frac{\mathrm{d}f(\eta)}{\mathrm{d}\eta}\right)^2\right] = 0, \tag{11}$$

which is known as the Falkner–Skan boundary-layer equation[1]. Boundary conditions of $f(\eta)$ are

$$\text{At } \eta = 0: \quad f(0) = \frac{\mathrm{d}f(0)}{\mathrm{d}\eta} = 0,$$

$$\text{At } \eta \to \infty: \quad \frac{\mathrm{d}f(\infty)}{\mathrm{d}\eta} = 1. \tag{12}$$

Note that in the above equations, parameters β and m are related through the expression $\beta = 2m/(m + 1)$. A dimensionless temperature is defined as follows

$$\theta = \frac{T - T_\infty}{T_w - T_\infty}. \tag{13}$$

If eq. (13) is substituted into eq. (5), the boundary-layer energy equation becomes

$$\frac{\mathrm{d}^2\theta(\eta)}{\mathrm{d}^2\eta} + Pr \cdot f(\eta, \beta) \cdot \frac{\mathrm{d}\theta(\eta)}{\mathrm{d}\eta} = 0, \tag{14}$$

with the following boundary conditions

$$\text{At } \eta = 0: \quad \theta = 1,$$

$$\text{At } \eta \to \infty: \quad \theta = 0, \tag{15}$$

where Pr is the Prandtl number, which is equal to the ratio of the momentum diffusivity of the fluid to its thermal diffusivity (i.e. $Pr = \upsilon/\alpha$). Equations (11) and (14) present a system of ordinary differential equations for the Falkner–Skan boundary-layer problem. Simultaneous solution of these two equations yields the velocity and temperature profiles for the flow of a viscous fluid passing over a wedge.

Analytical solution

For HAM solutions, we choose initial guesses and the auxiliary linear operator in the following form:

$$f_0(\eta) = \frac{1}{2}\alpha_1\eta^2, \quad \theta_0(\eta) = 1 + \alpha_2\eta, \tag{16}$$

$$L_1(f) = f''', \quad L_2(\theta) = \theta'', \tag{17}$$

$$L_1(c_1\eta^2 + c_2\eta + c_3) = 0, \quad L_2(c_4\eta + c_5) = 0. \tag{18}$$

And, c_i (i = 1–5) are constants. Let $p \in [0, 1]$ denote the embedding parameter and $\hbar_1, \hbar_2$ indicate the non-zero auxiliary parameters. We take $\hbar_1 = \hbar_2 = -1$ for the trial and error method and construct the following problems.

Zeroth-order deformation problems

$$(1-p)L_1[f(\eta, p) - f_0(\eta)] = p\hbar_1 N_1[f(\eta, p), \theta(\eta, p)], \tag{19}$$

$$f(0, p) = 0, \quad f'(0, p) = 0, \quad f''(0, p) = \alpha_1, \tag{20}$$

$$(1-p)L_2[\theta(\eta, p) - \theta_0(\eta)] = p\hbar_2 N_2[f(\eta, p), \theta(\eta, p)], \tag{21}$$

$$\theta(0, p) = 1, \quad \theta'(0, p) = \alpha_2, \tag{22}$$

$$N_1[f(\eta, p), \theta(\eta, p)] = \frac{\partial^3 f(\eta, p)}{\partial \eta^3} + \left(f(\eta, p) \frac{\partial^2 f(\eta, p)}{\partial \eta^2} \right) + \beta \left(1 - \left(\frac{\partial f(\eta, p)}{\partial \eta} \right)^2 \right), \tag{23}$$

$$N_2[f(\eta, p), \theta(\eta, p)] = \frac{\partial^2 \theta(\eta, p)}{\partial \eta^2} + Pr \left(f(\eta, p) \frac{\partial \theta(\eta, p)}{\partial \eta} \right). \tag{24}$$

For $p = 0$ and $p = 1$ we have

$$f(\eta, 0) = f_0(\eta), \quad f(\eta, 1) = f(\eta), \tag{25}$$

$$\theta(\eta, 0) = \theta_0(\eta), \quad \theta(\eta, 1) = \theta(\eta). \tag{26}$$

When p increases from 0 to 1, $f(\eta, p)$ and $\theta(\eta, p)$ vary from $f_0(\eta)$ and $\theta_0(\eta)$ to $f(\eta)$ and $\theta(\eta)$. According to the Taylor series with respect to p, we have

$$f(\eta, p) = f_0(\eta) + \sum_{m=1}^{\infty} f_m(\eta) p^m,$$
$$f_m(\eta) = \frac{1}{m!} \frac{\partial^m (f(\eta, p))}{\partial p^m}, \tag{27}$$

$$\theta(\eta, p) = \theta_0(\eta) + \sum_{m=1}^{\infty} \theta_m(\eta) p^m,$$
$$\theta_m(\eta) = \frac{1}{m!} \frac{\partial^m (\theta(\eta, p))}{\partial p^m}. \tag{28}$$

$\hbar_1$ and $\hbar_2$ are chosen in such a way that these two series are convergent at $p = 1$. Therefore, we have through eqs (27) and (28)

$$f(\eta) = f_0(\eta) + \sum_{m=1}^{\infty} f_m(\eta), \quad \theta(\eta) = \theta_0(\eta) + \sum_{m=1}^{\infty} \theta_m(\eta). \tag{29}$$

mth-order deformation problems

$$L_1[f_m(\eta) - \chi_m f_{m-1}(\eta)] = \hbar_1 R_m^f(\eta), \tag{30}$$

$$f_m(0) = f_m'(0) = f_m''(0) = 0, \tag{31}$$

$$L_2[\theta_m(\eta) - \chi_m \theta_{m-1}(\eta)] = \hbar_2 R_m^\theta(\eta), \tag{32}$$

$$\theta_m(0) = \theta_m'(0) = 0, \tag{33}$$

$$R_m^f = f_{m-1}''' + \sum_{n=0}^{m-1} f_{m-1-n} f_n'' + \beta(1 - f'^2), \tag{34}$$

$$R_m^\theta = \theta_{m-1}'' + Pr \sum_{n=0}^{m-1} f_{m-1-n} \theta_n', \tag{35}$$

$$\chi_m = \begin{cases} 0 & \text{for } m \le 1, \\ 1 & \text{for } m > 1, \end{cases} \tag{36}$$

where the differential operators L_1, L_2 are given by

$$L_1 = \frac{\mathrm{d}^3}{\mathrm{d}\eta^3}, \; L_2 = \frac{\mathrm{d}^2}{\mathrm{d}\eta^2};$$

we also assume that the inverse of the operators L_1, L_2 exists, which can be integrated from 0 to η, i.e.

$$L_1^{-1} = \int_0^\eta \int_0^\eta \int_0^\eta \mathrm{d}\eta \mathrm{d}\eta \mathrm{d}\eta \quad \text{and} \quad L_2^{-1} = \int_0^\eta \int_0^\eta (.) \mathrm{d}\eta \mathrm{d}\eta.$$

For the prediction of α_1, different analytical models were presented by Wang[23] and Hashim[24]. In the present study trail and error is used to consider the physical meaning of f' and f'' in the boundary layer as used by Abbasbandy[25]. Therefore, to consider the infinite boundary condition of eq. (18), $\eta \to \infty$: $f' = 1$ and recall that f' is the dimensionless velocity inside the boundary layer and f'' is related to the shear stress. Then, η can be determined when f'' approaches zero outside the boundary layer. Therefore, the value of η is very large while that of f'' is very small. To assume a new variable η_∞, we have $\eta \to \infty$: $f'' = 0$. Consequently, we would have two nonlinear algebraic equations with variables α_1 and η, that can be solved using the trail and error method. Two nonlinear algebraic equations are presented as

$$\eta \to \infty: \; f' = 1, \quad \eta \to \infty: \; f'' = 0. \tag{37}$$

The Padé approximation

This section is concerned with the mathematical behaviour of the solution $\theta(\eta)$ in order to determine $\theta'(0) = \alpha_2$. It was shown by some authors that this can be achieved by forming Padé approximations[26] which have the advantage of manipulating the polynomial approximation into a rational function to gain more information about $\theta(\eta)$. It is well known that Padé approximations will converge on the entire real axis[27], if $\theta(\eta)$ is free of singularities on the real axis. Moreover, it should to be noted that

Table 2. Numerical values of $\theta'(\eta)$ for various Prandtl numbers (Pr) and wedge angle parameters

	$\theta'(\eta)$					
	$\beta = 0$		$\beta = 0.3$		$\beta = 2.0$	
Pr	Present study	White[28]	Present study	White[28]	Present study	White[28]
0.1	0.1974	0.1980	0.2101	0.2090	0.2264	0.2260
0.3	0.3054	0.3037	0.3290	0.3278	0.3626	0.3668
0.6	0.3923	0.3916	0.4290	0.4289	0.4890	0.4913
0.72	0.4183	0.4178	0.4596	0.4592	0.5277	0.5292
1.0	0.4696	0.4696	0.5195	0.5195	0.6030	0.6052
2.0	0.7972	0.5972	0.6690	0.6690	0.7944	0.7959
3.0	0.6858	0.6859	0.7737	0.7739	0.9283	0.9303
6.0	0.8668	0.8672	0.9885	0.9872	1.2067	1.2069
10.0	1.0283	1.0297	1.1781	1.1791	1.4553	1.4557
30.0	1.4813	1.4873	1.7199	1.7198	2.1603	2.1577
60.0	1.8759	1.8746	2.1777	2.1776	2.7493	2.7520
100.0	2.2229	2.2229	2.5890	2.5892	3.2821	3.2863
400.0	3.5319	3.5292	4.1338	4.1331	5.2842	5.2890
1,000.0	4.7900	4.7901	5.6228	5.6230	7.2209	7.2212
4,000.0	7.6093	7.6039	8.9481	8.9481	11.524	11.532
10,000.0	10.342	10.320	12.160	12.157	15.6853	15.692

Padé-finding algorithms are built-in utilities in most manipulation languages[27], such as Maple and Mathematica. More importantly, the diagonal approximation is the most accurate approximation; therefore we will construct only the diagonal approximations in the following discussions. Using the boundary condition $\theta(\infty) = 0$, the diagonal approximation $[M/M]$ vanishes if the coefficient of η with the highest power vanishes. We obtain 31 approximate terms of $\theta(\eta)$, which are given as

$$\sum_{i=0}^{30} \theta_i(\eta) = \theta_{31}(\eta).$$

The values of α_2 can be calculated using conditions at the unbounded domain

$$\lim_{\eta\to\infty} \theta_{31}(\eta)[M/M] = 0,$$

and the diagonal approximation. Using the Maple built-in utilities to solve the resulting polynomials gives the values of $\theta'(0)$ listed in Table 2. These values compare well with the highly accurate numerical solution provided by White[28].

In applying the boundary condition $\theta(\infty) = 0$ to the diagonal approximations, a polynomial equation for α is obtained, which gives many roots, while eq. (14) has a unique solution so only the real and physical root must be chosen for simulations.

We provide the solution as

$$f_1(\eta) = \frac{-1}{120}\alpha_1{}^2\eta^5 - \frac{1}{6}\beta\eta^3 + \frac{1}{60}\beta\alpha_1{}^2\eta^5, \tag{38}$$

$$\theta_1(\eta) = \frac{-1}{24} Pr\cdot\alpha_1\alpha_2\eta^4, \tag{39}$$

$$f_2(\eta) = \frac{11}{40,320}\alpha_1^3\eta^8 + \frac{1}{80}\alpha_1\beta\eta^6 - \frac{1}{1260}\beta\alpha_1^3\eta^8 + \frac{1}{2016}\beta^2\alpha_1^3\eta^8 - \frac{1}{120}\beta^2\alpha_1\eta^6, \tag{40}$$

$$\theta_2(\eta) = \frac{-1}{5040} Pr\cdot\alpha_2\eta^5 \times\left(-\alpha_1^2\eta^2 - 42\beta + 2\beta\alpha_1^2\eta^2 - 10Pr\cdot\alpha_1^2\eta^2\right), \tag{41}$$

$$f_3(\eta) = \frac{-5}{532,224}\alpha_1^4\eta^{11} - \frac{1}{4032}\alpha_1^2\beta\eta^9 + \frac{233}{6,652,800}\beta\alpha_1^4\eta^{11} - \frac{19}{475,200}\beta^2\alpha_1^4\eta^{11} + \frac{113}{181,440}\beta^2\alpha_1^2\eta^9 - \frac{1}{1260}\beta^2\eta^7 + \frac{1}{66,528}\beta^3\alpha_1^4\eta^{11} - \frac{11}{30,240}\beta^3\alpha_1^2\eta^9 + \frac{1}{840}\beta^3\eta^7, \tag{42}$$

$$\theta_3(\eta) = \frac{-1}{3,628,800} Pr\cdot\alpha_2\alpha_1\eta^8 \times\begin{pmatrix} \alpha_1^2\eta^2 + 360\beta - 32\beta\alpha_1^2\eta^2 + 20\beta^2\alpha_1^2\eta^2 \\ -540\beta^2 + 84Pr\cdot\alpha_1^2\eta^2 - 168Pr\cdot\beta\alpha_1^2\eta^2 \\ +3150Pr\cdot\beta + 280Pr^2\cdot\alpha_1^2\eta^2 \end{pmatrix}. \tag{43}$$

Numerical results and discussion

This study considered a thermal boundary-layer problem in the case of a two-dimensional incompressible flow passing over a wedge, with the assumption of constant physical properties with temperature. The momentum equation is decoupled from the energy equation. Therefore, the results are presented in two sections – velocity and thermal boundary layers.

Velocity boundary layer

The velocity profiles $f'(\eta)$ for different values of β (or equivalently m) are given in Figure 2. For accelerated flows ($m > 0$, $\beta > 0$), we obtain velocity profiles without a point of inflection; for retarded flows ($m < 0$, $\beta < 0$), we obtain profiles with a point of inflection. Some important special cases are the flat plate flow ($m = 0$) and the stagnation point flow ($m = 1$). The case $m = 1/3$, $\beta = 1/2$ is worthy of attention. In this case the differential equation for $f(\eta)$ becomes: $f''' + ff'' + \frac{1}{2}(1 - f'^2) = 0$; it is transformed into the differential equation of rotationally symmetrical flow with stagnation point, i.e. $\phi''' + 2\phi\phi'' + (1 - \phi'^2) = 0$ for $\phi(\xi)$, if we put $\eta = \xi\sqrt{2}$ and $df/d\eta = d\phi/d\xi$ (ref. 29). This means that the calculation of boundary layer in the rotationally symmetrical case can be reduced to the calculation of two-dimensional flow past a wedge[29] whose included angle is $\beta\pi = \pi/2$ The case $m = -0.091$, $\beta = -0.199$ corresponds to the velocity profile with vanishing wall shear stress (separation). From the small numerical value $m = -0.091$, we see that the laminar boundary layer can only withstand a very small retardation of the flow (or equivalently a very small adverse pressure gradient) before separation takes place.

Table 3 presents a comparison of the current numerical results of $f''(0) = \alpha_1$ for various values of β with those presented by Rajagopal *et al.*[4] and Kuo[9]. It can be noted that there is good agreement between three sets of results. Table 1 shows the degree of Padé approximations for the case of the flat plate to illustrate the efficiency of these approximations. An important conclusion can be drawn that the error decreases dramatically with the increase in the degree of the Padé approximations. The error has been calculated using the highly accurate numerical solution provided by White[28] as: $f''(0) = 0.46960$.

Table 3. Comparison of the results for the laminar boundary layer over a wedge

	$f''(0)$		
β	Present method	Rajagopal *et al.*[4]	Bor-Lih Kuo[9]
0.0	0.4683	0.4696	0.4696
0.05	0.5314	0.5311	0.5317
0.1	0.5879	0.5870	0.5878
0.2	0.6873	0.6867	0.6876
0.3	0.7746	0.7747	0.7755
0.4	0.8536	0.8544	0.8549
0.5	0.9262	0.9276	0.9279
0.6	0.9940	0.9958	0.9957
0.7	1.058	****	1.0590
0.8	1.1188	1.1202	1.1195
0.9	1.1764	****	1.1767
1.0	1.2313	1.2325	1.2312
1.2	1.3334	1.3357	1.3338
1.6	1.52067	1.5215	1.5184
2.0	1.6865	****	1.6830
–0.199	0.035	****	****
–0.14	0.2481	****	****

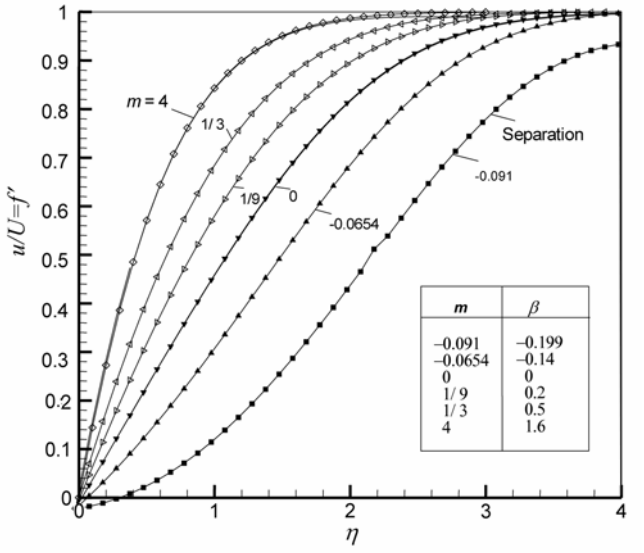

Figure 2. Velocity distribution in the laminar boundary layer of the wedge flow. The lines show the homotopy analysis method (HAM) and symbols show the numerical solution[29].

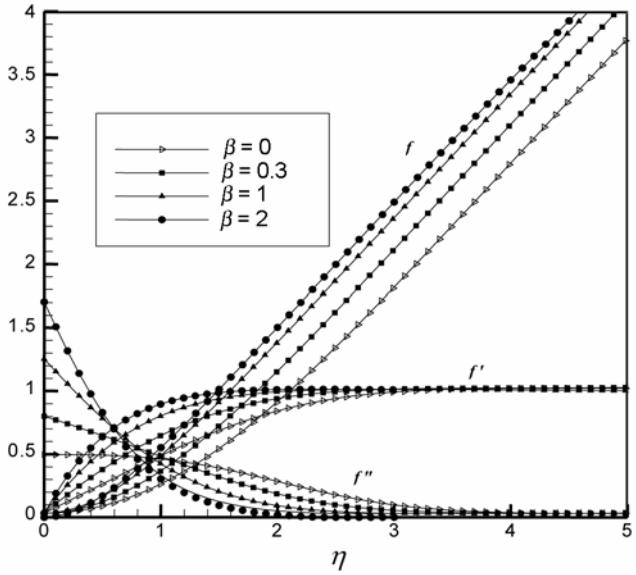

Figure 3. Numerical results of $f(\eta)$ and its derivatives for various values of β.

Figure 3 is a plot of the variation in the values of $f(\eta)$ and its derivatives for various values of β. The results obtained by the present method are in good agreement with those provided by White[28]. The results indicate that steeper velocity profiles are associated with larger values of the wedge angle parameter β. As β is a measure of the pressure gradient, a positive value of β indicates a negative (or favourable) pressure gradient. For accelerated flows (i.e. positive values of β), the f' profiles merely squeeze closer and closer to the wall, and overshoot or backflow phenomena are not noted.

It should be mentioned that the difference between numerical and HAM solutions depends on the number of HAM terms (Figure 4). In the present work, the analytical result shows that the HAM solution with ten terms has good agreement with the numerical solution, with a high rate of convergence as well.

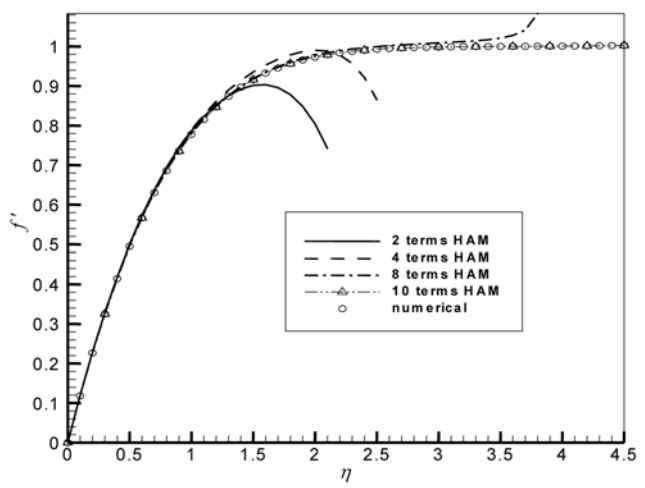

Figure 4. The velocity boundary layer of the wedge with $\beta = 0$ and $m = 0$.

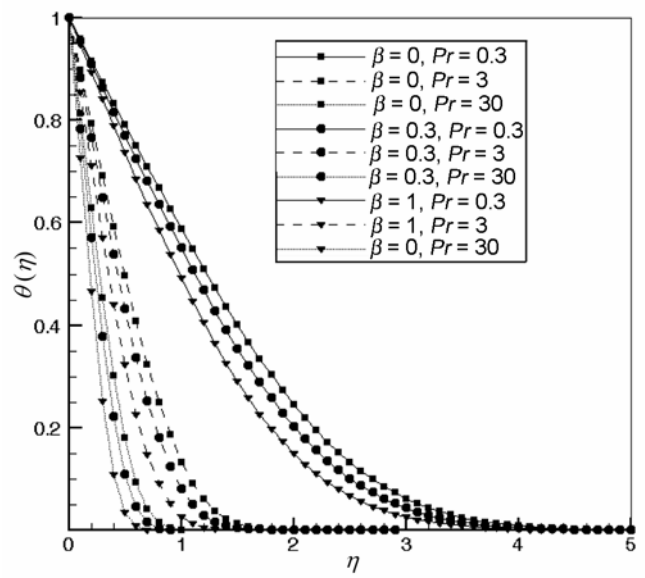

Figure 5. Dimensionless temperature profiles for various values of β and Prandtl number.

Thermal boundary layer

Figure 5 shows the dimensionless temperature profiles for various values of β and *Pr*. It can be noted that the maximum difference in the dimensionless temperature distributions for various values of β occurs at larger values of *Pr* and that this difference decreases as *Pr* decreases.

Figure 6 is a plot of the dimensionless temperature distributions of the Falkner–Skan boundary-layer problem for the *Pr* range 0.006–10,000.

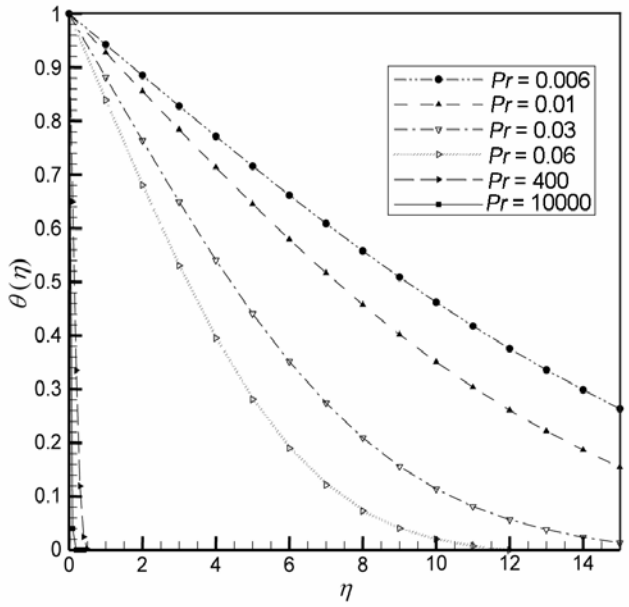

Figure 6. Dimensionless temperature profiles for $\beta = 0$ and various Prandtl numbers.

Table 4. Padé approximations and $\theta'(0)$

Padé approximation	$\beta = 0$, $Pr = 0.72$	$\beta = 0.3$, $Pr = 3$
[2/2]	0.2	0.25
[3/3]	0.5522	1.352
[4/4]	0.43	0.9854
[7/7]	0.4122	0.6553
[10/10]	0.4184	0.7907
[12/12]	0.4179	0.8677
[13/13]	0.4183	0.7640
[14/14]	0.4183	0.7640
[15/15]	0.4183	0.7780
[19/19]	****	0.7730
[21/21]	****	0.7735
[23/23]	****	0.7734
[24/24]	****	0.7734
[25/25]	****	0.7734
[26/26]	****	0.7734

Table 2 presents a comparison of the current numerical results of $\theta'(0)$ for different values of β and Pr with those presented by White[28]. Once again, it is seen that there is good agreement between the two sets of results. Table 4 presents values of $\theta'(0) = \alpha_2$ which can be calculated by the Padé approximation method for two different values of β and Pr. It can be concluded that higher degree of the Padé approximations provides a highly accurate value of $\theta'(0)$ compared to that presented by White[28].

Conclusion

The fundamental goal of this work has been to establish an analytical solution to obtain the temperature distributions for a flow passing over a wedge. This has been achieved using HAM.

There are three important points to note here. First, the methodology used so far applies perturbative methods or variational principles that mostly lead to complicated integrals involving Green and Error functions. Further, the accuracy level can be dramatically enhanced by computing further components of $f(\eta)$, $\theta(\eta)$. Second, the behaviour of the model, in that it decreases rapidly to extinction in the long run, can be formally determined using the Padé approximation. Further, combining the series obtained with the Padé approximation provides a promising tool to handle problems on an unbounded domain. The Padé approximations, that often show superior performance over series approximations, provide a promising tool for use in scientific applications. Finally, it should be noted that the approximation obtained for the value of $f''(0) = \alpha_1$ which is calculated by the trial and error method is a good one, with minimal error when compared to other studies. Accurate approximation for $f''(0)$ can be easily obtained using the built-in utilities in Maple and Mathematica. These advantages demonstrate the reliability and efficiency of the method. It has been demonstrated that the obtained analytical results for the velocity and temperature distributions are in excellent agreement with those provided by other numerical approximation methods.

Nomenclature

L_1, L_2	Operator of the highest-order derivative
L_1^{-1}, L_2^{-1}	Inverse operator of L_1, L_2
N	Nonlinear operator
τ	Independent variable
T	Temperature (°C)
T_w	Wall temperature (°C)
T_∞	Temperature of free stream (°C)
Pr	Prandtl number (υ/α)
f_x	Body force in Navier–Stokes equation
U_∞	Velocity of free stream (m/s)
x	Dimensional space coordinate
$\hbar$	Auxiliary parameter
$H(\tau)$	Auxiliary function
$p \in [0, 1]$	Embedding parameter

Greek symbols

θ	Dimensionless temperature $(T - T_\infty)/(T_w - T_\infty)$
α_1	The value of f'' at $\eta = 0$
α	Thermal diffusivity ($k/\rho c_p$)
α_2	Temperature profile gradient at $\eta = 0$, namely $\theta'(0)$
υ	Kinematic viscosity (m^2/s)
η	Dimensionless variable similarity solution
ψ	Stream function

Subscripts

m	Power of length coordinate, x, of the velocity of the potential flow, $U(x) = U_\infty(x/L)^m$
m, n	Number of terms in the series

1. Falkner, V. M. and Skan, S. W., Some approximate solutions of the boundary layer equations. *Philos. Mag*., 1931, **12**, 865–896.
2. Hartree, D. H., On an equation occurring in Falkner and Skan's approximate treatment of the equations of the boundary layer. *Proc. Cambridge Philos. Soc*., 1937, **33**, 223–239.
3. Na, T. Y., *Computational Methods in Engineering Boundary Value Problems*, Academic Press, New York, 1979.
4. Rajagopal, K. R., Gupta, A. S. and Na, T. Y., A note on the Falkner–Skan flows of a non-Newtonian fluid. *Int. J. Non-Linear Mech*., 1983, **18**, 313.
5. Lin, H. T. and Lin, L. K., Similarity solutions for laminar forced convection heat transfer from wedges to fluids of any Prandtl number. *Int. J. Heat Mass Transfer*, 1987, **30**, 1111.
6. Hsu, C. H., Chen, C. S. and Teng, J. T., Temperature and flow fields for the flow of a second grade fluid past a wedge. *Int. J. Non-Linear Mech*., 1997, **32**, 933–946.
7. Asaithambi, A., A finite-difference method for the solution of the Falkner–Skan equation. *Appl. Math. Comput*., 1998, **92**, 135–141.
8. Hsu, C. H. and Hsiao, K. L., Conjugate heat transfer of a plate fin in a second-grade fluid flow. *Int. J. Heat Mass Transfer*, 1998, **41**, 1087–1102.
9. Kuo, Bor-Lih, Transfer analysis for the Falkner–Skan wedge flow by the differential transformation method. *Int. J. Heat Mass Transfer*., 2005, **48**, 5036–5046.
10. Liao, S. J., The proposed homotopy analysis technique for the solution of nonlinear problems. Ph D thesis, Shanghai Jiao Tong University, China, 1992.
11. Liao, S. J., *Beyond Perturbation: Introduction to the Homotopy Analysis Method*, Chapman & Hall/CRC Press, Boca Raton, 2003.
12. Liao, S. J. and Cheung, K. F., Homotopy analysis of nonlinear progressive waves in deep water. *J. Eng. Math*., 2003, **45**, 103–116.
13. Liao, S. J., Series solutions of unsteady boundary-layer flows over a stretching flat plate. *Stud. Appl. Math*., 2006, **17**, 239–264.
14. Ghasemi, E., Soleimani, S., Barari, A., Bararnia, H. and Domairry, G., The influence of uniform suction/injection on heat transfer of MHD Hiemenz flow in porous media. *J. Eng. Mech*., *ASCE*, 2012, **138**, 82–88.
15. Ghotbi, A. R., Omidvar, M. and Barari, A., Infiltration in unsaturated soils – An analytical approach. *Comput. Geotech*., 2011, **38**, 777–782.

16. Hayat, T., Khan, M. and Ayub, M., On non-linear flows with slip boundary condition. *Z. Angew., Math. Phys*., 2005, **56**, 1012–1029.
17. Hayat, T., Abbas, Z., Sajid, M. and Asghar, S., The influence of thermal radiation on MHD flow of a second grade fluid. *Int. J. Heat Mass Transfer*., 2007, **50**, 931–941.
18. Hayat, T., Sajid, M. and Pop, I., Three dimensional flow over a stretching surface in a viscoelastic fluid. *Nonlinear Anal.: Real World Appl.*, 2008, **9**, 1811–1822.
19. Barari, A., Kimiaeifar, A., Domairry, G. and Moghimi, M., Analytical evaluation of beam deformation problem using approximate methods. *Songklanakarin J. Sci. Technol.*, **32**, 281–288.
20. Momeni, M., Jamshidi, N., Barari, A. and Domairry, G., Numerical analysis of flow and heat transfer of a viscoelastic fluid over a stretching sheet by using the homotopy analysis method. *Int. J. Num. Methods Heat Fluid Flow*, 2011, **21**, 206–218.
21. Ghotbi, A. R., Bararnia, H., Domairry, G. and Barari, A., Investigation of a powerful analytical method into forced and natural convection boundary layer flow. *Int. J. Commun. Nonlinear Sci. Numer. Simul.*, 2009, **14**, 2222–2228.
22. Parand, K., Shahini, M. and Dehghan, M., Solution of a laminar boundary layer flow via a numerical method. *Commun. Nonlinear Sci. Numer. Simul.*, 2010, **15**, 360–367.
23. Wang, L., A new algorithm for solving classical Blasius equation. *Appl. Math. Comput*., 2004, **157**, 1–9.
24. Hashim, I., Comments on A new algorithm for solving classical Blasius equation by L. Wang. *J. Appl. Math. Comput.*, 2006, **176**, 700–703.
25. Abbasbandy, S. A., A numerical solution of Blasius equation by Adomian's decomposition method and comparison with homotopy perturbation method. *Chaos Solitons Fract*., 2007, **31**, 257–260.
26. Baker, G. A., *Essentials of Padé Approximants*, Academic Press, London, 1975.
27. Boyd, J., Padé approximant algorithm for solving nonlinear ordinary differential equation boundary value problems on an unbounded domain. *Comput. Phys*., 1997, **11**, 299–303.
28. White, F. M., *Viscous Fluid Flow*, McGraw-Hill, New York, 1991, 2nd edn, pp. 242–249.
29. Schilichting, H., *Boundary-layer Theory*, McGraw-Hill, New York, 2004, 8th edn.

Received 23 July 2011; revised accepted 15 June 2012